RADIOCARBON, Vol 49, Nr 2, 2007, p 233–244

INTEGRATING CONTINUOUS-FLOW MASS SPECTROMETRY AND AUTOMATIC CO_2 COLLECTION FOR AMS

Jesper Olsen[1,2] • Jan Heinemeier[1] • Klaus Bahner[1] • Barry Graney[3] • Andy Phillips[3]

ABSTRACT. Accelerator mass spectrometry (AMS) radiocarbon measurements of organic samples require combustion to obtain CO_2 for graphitization. Furthermore, determination of $\delta^{13}C$ values is required in order to correct the ^{14}C age due to carbon isotope fractionation effects. $\delta^{13}C$ analysis is commonly carried out by stable isotope mass spectrometry because most applications demand high-precision $\delta^{13}C$ values in addition to the requirements of ^{14}C dating. A simplifying step is therefore to combine the combustion for stable isotope analysis with cryogenic trapping of CO_2 for AMS graphite targets. Presented here is a simple CO_2 trapping device based on a modified Gilson 220XL sampling (manifold) robot coupled to the inlet manifold system of a GV Instruments IsoPrime stable isotope mass spectrometer. The system is capable of batch combustion and analysis of up to 40 samples and is under full computer control by the mass spectrometer software. All trapping parameters such as flush time prior to trapping and total trap time are adjustable through the standard software user interface. A low ^{14}C activity of background materials and high precision and accuracy of stable isotope analysis of carbon and nitrogen are demonstrated.

INTRODUCTION

Radiocarbon measurements by accelerator mass spectrometry (AMS) of organic samples require combustion to obtain CO_2 for graphitization, and commonly a fraction of the produced CO_2 is further analyzed by stable isotope mass spectrometry for the determination of precise $\delta^{13}C$ values. Usually, samples for ^{14}C analysis are, after pretreatment procedures, combusted off-line in sealed, evacuated tubes containing CuO. Afterwards, the produced CO_2 is manually transferred to the graphitization system and a small aliquot is stored for stable isotope $\delta^{13}C$ analysis. $\delta^{13}C$ measurements are mandatory for ^{14}C measurements in order to correct for fractionation (Stuiver and Polach 1977; McNichol et al. 2001). A simplifying step is therefore to combine the combustion in a continuous-flow elemental analyzer (CF-EA) stable isotope ratio mass spectrometer (IRMS) with cryogenic trapping of CO_2 for AMS graphite targets. Automated or semi-automated trapping devices for CO_2 coupled to elemental analysis continuous-flow isotope mass spectrometers have previously been described (see e.g. Bronk Ramsey and Humm 2000; Morgenroth et al. 2000; Aerts-Bijma et al. 2001; Hatté et al. 2003). A fully automated system integrated into the mass spectrometer equipment and software has not yet been reported. Furthermore, the combination of CF-EA analysis and CO_2 trapping additionally provides determination of $\delta^{15}N$. Many studies require the measurement of both $\delta^{13}C$ and $\delta^{15}N$ as it is often used in paleodietary studies (Leach et al. 2001; Ambrose and Krigbaum 2003; Richter and Noe-Nygaard 2003; Newsome et al. 2004; Noe-Nygaard et al. 2005), but also for analyzing plant material used in climate or ecological research (Ghosh and Brand 2003; Filippi and Talbot 2005; Kohn and Law 2006; Talbot et al. 2006).

An automated sample gas preparation device for ^{14}C samples coupled to a mass spectrometer has been developed based on a Gilson 220XL sampling robot, modified to serve as a simple CO_2 cryogenic trapping device. A small dewar, automatically held at a constant level of liquid nitrogen, is added to the existing Gilson robot arm, ensuring that the CO_2 samples for graphitization are trapped in small, septum-sealed vials. The Gilson is operated with a dual-carriageway needle to ensure a

[1]Department of Physics and Astronomy, Aarhus University, DK-8000 Aarhus C, Denmark.
[2]Department of Earth Sciences, Aarhus University, DK-8000 Aarhus C, Denmark. Corresponding author.
Email: jesper.olsen@geo.au.dk.
[3]GV Instruments, Crewe Road, Wythenshawe, Manchester M23 9BE, United Kingdom.

Proceedings of the 19th International ^{14}C Conference, edited by C Bronk Ramsey and TFG Higham
RADIOCARBON, Vol 49, Nr 2, 2007, p 233–244

constant helium flow at all times and to let the sample CO_2 into the trapping vials. The system is capable of batch combustion and isotope analysis of up to 40 samples and is under full computer control by the mass spectrometer software. The very first results obtained on our prototype setup are presented below.

METHOD AND DESIGN

Previous designs of automated sample preparation for AMS samples suffered either from being semi-automatic or from being very large and in general disconnected from the mass spectrometer software commonly controlling the CF-EA sample combustion sequence (Bronk Ramsey and Humm 2000; Aerts-Bijma et al. 2001; Hatté et al. 2003). Therefore, in order to improve the automation technique, our demands for the design of the automated AMS sample preparation system were that it should be fully integrated and compatible with the IRMS equipment. Furthermore, it should be simple, easily operated, and straightforward to set up. The last point is especially important as most IRMS are capable of connecting to a variety of inlet systems, i.e. CF-EA carbon and nitrogen, CF-EA sulphur, CF-EA hydrogen, and dual-inlet analysis (see e.g. Werner and Brand 2001).

For routine $\delta^{13}C$ and $\delta^{18}O$ analysis on off-line-prepared CO_2 samples, a Gilson robot 220XL with its 50-sample manifold bed is operated to transfer the CO_2 samples from spring-loaded sample vials to the dual inlet for stable isotope analysis. To the existing Gilson robot arm, a 90-degree rotated U extension arm holding a dewar is added (see Figure 1). The dewar is positioned directly below the needle and is placed on a threaded spindle, which is driven by a motor drive in order to move the dewar vertically. A slide is fixed to the bottom of the U-formed extension, to which a vertical holder is placed. The vertical holder is attached to the end of the existing Gilson robot arm. The slide and a wheel placed on the vertical holder allow the Gilson to move freely in the *x* and *y* direction (see Figure 1) without adding extra weight to the existing Gilson robot arm. The extension robot arm is constructed in aluminium and is made as light and rigid as possible and can be readily removed from the Gilson robot at the assembly points (Figure 1).

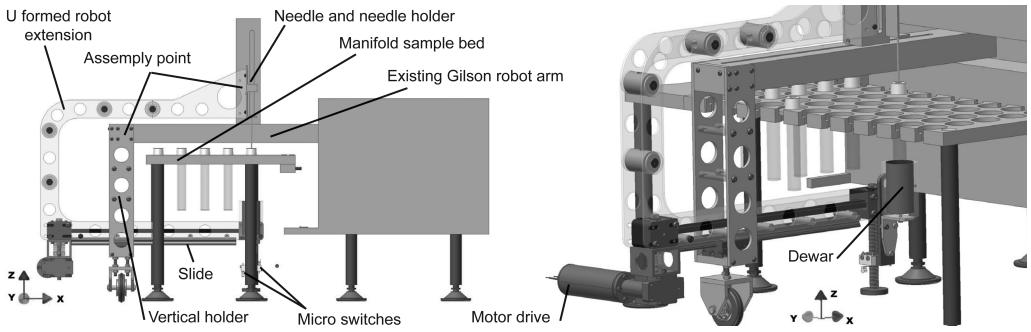

Figure 1 Modified Gilson 220XL and design of the robot extension arm (CAD drawing by Henrik Bechthold, Department of Physics and Astronomy [Construction], University of Aarhus).

The integrated system consists of a modified continuous-flow elemental analyzer (CF-EA) (EuroVector 3024) producing gaseous N_2 and CO_2 from solid samples loaded into tin cups, a modified Gilson 220XL for cryogenic CO_2 trapping, and an isotope ratio mass spectrometer (IRMS) (GV Instruments IsoPrime) as illustrated in Figure 2. The system is controlled by the IRMS computer. The CF-EA is modified as outlined by Aerts-Bijma et al. (2001). However, in contrast to Aerts-Bijma et al. (2001), an adjustable needle valve has been added to the IRMS line of the modified CF-

EA to dilute the carrier helium flow and to reduce the amount of sample entering the IRMS detectors (see Figure 2). The stable isotopes are converted to the VPDB scale for $\delta^{13}C$ values and the AIR scale for $\delta^{15}N$ values using standard procedures (Craig 1957; Allison et al. 1993; Werner and Brand 2001).

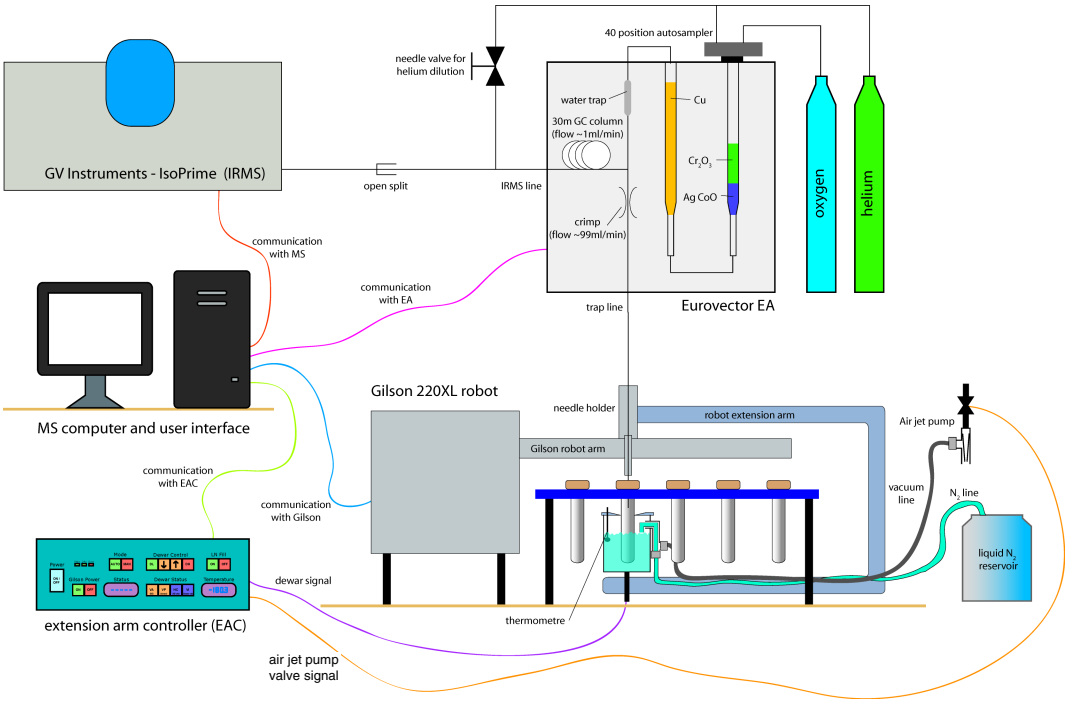

Figure 2 Schematics of the CF-EA-AMS automated sample preparation system

The CO_2 produced by the CF-EA system is transferred to septum-sealed sample vials via a double-carriageway needle (Figure 3), maintaining a continuous carrier flow at all times. A small vial insert containing a second septum (Figure 3) has been developed to ensure that the CO_2 is transferred to the cold region at the bottom of the vial for cryogenic trapping. The injection needle first penetrates the vial septum sealing to atmosphere and only the needle tip penetrates the vial insert septum while the gas outlet stays between the septa. The dewar is made of stainless steel and its side wall and bottom is isolated by 5-mm polytetrafluoroethylene (PTFE). A stainless steel disk with a hole matching the diameter of the sample vials is placed at the top of dewar. The disk hole is sleeved to provide vial guidance. When the dewar is at its upward position, the dewar interior is a closed system into which liquid nitrogen is transferred by an air jet pump producing vacuum (Figure 2). Both the dewar position and the air jet pump are controlled by an additional extension arm controller (EAC; see Figure 2).

The main function of the extension arm controller (EAC) is to control the dewar motor drive (dewar position) and the liquid nitrogen filling by measuring the dewar temperature and controlling the air jet pump valve (Figure 2) as well as to provide a communication interface to the IRMS software. The dewar position is controlled by 2 microswitches. The EAC may be operated remotely by the IRMS software or manually for adjustments and testing. The communication with the IRMS software is provided by 4 Boolean signals: 2 for activating the liquid nitrogen filling and the dewar position, respectively, and 2 for reporting the status of the dewar position and temperature.

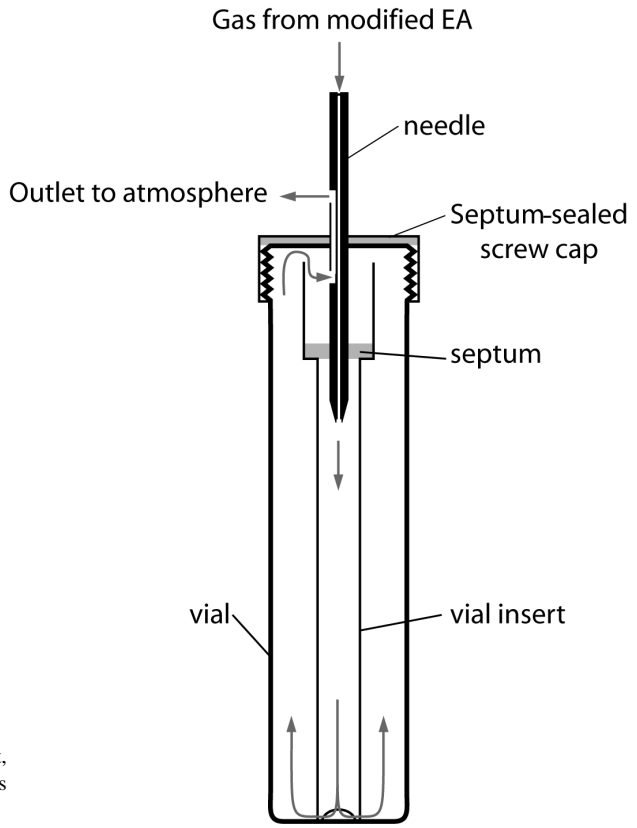

Figure 3 Schematics of the vial, vial insert, and dual-carriageway needle. The gas flow is indicated by the arrows.

The IRMS software script ensures that prior to the CF-EA sample drop, the vial is fully flushed with helium and the dewar is raised to its upper position and cooled. Before letting the Gilson move to the sample position, the status of the dewar position and N_2 filling is checked. Thus, if and only if the dewar is at its lower position and the nitrogen filling is off, the Gilson goes to the sample vial, injects the needle, and flushes the vial with carrier helium. Then, the IRMS requests the EAC to raise the dewar. When the dewar is in its upper position, the liquid nitrogen filling is initiated. When the EAC signals the IRMS software that the dewar has reached an appropriate temperature, the sample is dropped into CF-EA combustion tube. After the trap time has passed, the IRMS commands the EAC to terminate the liquid nitrogen filling and to lower the dewar. When the dewar is at its lower position, the Gilson withdraws the needle and returns to its home position, ready for the next sample.

During analysis and CO_2 trapping, error handling is performed solely by the IRMS software through the Gilson robot error state. Furthermore, the Gilson main power is controlled by the EAC in order to avoid returning power to the Gilson after electric power failures, which potentially could damage the Gilson robot or the robot extension if the dewar is at the upper position. The EAC commands are accessible from the IRMS user interface and further enable the user to set the needle vertical position, the vial flush time, and the cryogenic trap time together with all other commonly available common parameters of CF-EA IRMS analysis.

RESULTS AND DISCUSSION

The freezing procedure, the AMS ^{14}C background level, and the stable isotope analysis of the CF-EA-AMS method have been investigated and are discussed below.

Freezing Procedure

For successful cryogenic trapping of the produced CO_2 gas, it is essential that the vial bottom temperature is below the CO_2 freezing point during the entire trapping time. Optimal parameters of the trapping procedure have been found by an iterative process of trial and error while monitoring the temperature of both the dewar and the vial. For the first ~60 seconds, the vial and dewar drops rapidly in temperature to about –180 °C, where it stabilizes. The temperature is then maintained below –160 °C by sequentially pumping liquid nitrogen into the dewar, and even though the dewar temperature fluctuates by approximately 20–30 °C, the vial temperature remains fairly constant at –180 °C. To ensure that the sample drop into the CF-EA combustion furnace is independent of the time used to cool the dewar, it is required that the dewar temperature must stay below –160 °C for a minimum of 20 s before the EAC signals the IRMS software to initiate the sample drop.

^{14}C Analysis—Background and Memory Effects

A batch of 19 ^{14}C standards in total are analyzed with the CF-EA-AMS preparation device (Table 1 and Figure 4) for determination of possible ^{14}C intersample memory effects. Two samples failed both stable isotope analysis and CO_2 trapping, and one further sample failed CO_2 trapping but was successfully analyzed for $\delta^{13}C$. These samples failed due to malfunction of the injection needle. During analysis, small fragments of septum rubber are stuck within the needle inlet cylinder, thus partially blocking the helium flow. Hence, for successful CO_2 trapping and stable isotope analysis the needle was cleaned for every second sample.

The ^{14}C analysis is among other things sensitive to the ^{14}C background level and to memory effects caused by the CF-EA system (Aerts-Bijma et al. 2001; Olsen et al. 2006). Aerts-Bijma et al. (2001) demonstrated that the position of the T-split for dividing the gas flow to the IRMS and the trapping device is crucial in order to minimize memory effects. Likewise, the CF-EA chemicals may also lead to memory effects. Intersample memory effects of the type reported by Aerts-Bijma et al. (2001) on their modified CF-EA trapping system were not detected, as observed from Table 1 and Figure 4.

It is commonly acknowledged that contamination with modern carbon is mainly induced by combustion and increases with smaller sample size (see e.g. Brown and Southon 1997; Morgenroth et al. 2000; Mueller and Muzikar 2002a,b; Hua et al. 2004), yielding the following formula:

$$pMC = \frac{C_1}{mass} + C_2$$

The constants C_1 and C_2 depend on the preparation and the term *mass* is the sample mass. Figure 5 shows the anthracite samples versus their inverse mass together with a linear fit to the data (apart from 1 obvious outlier). Firstly, the intercept with the pMC axis (Figure 5) indicates a mass-independent contamination with a ^{14}C activity of 0.12 ± 0.02 pMC (approximately 1 µg modern carbon) is added to the samples during CF-EA-AMS combustion and graphitization. Secondly, an additional contamination proportional to the inverse sample mass is added corresponding to a ^{14}C activity of 0.129 ± 0.009 pMC per mg C. The latter contamination effect is likely to be added during the graphitization step or inherent to the sample itself. Possibly, a mass-dependent contamination may also stem from the ion source sputter process due to a minor amount of evaporated oil from the diffusion

Table 1 Batch run of ^{14}C standards to test for possible intersample memory effects. The pMC values are not corrected for background level. The stable isotope $\delta^{13}C$ values are normalized by using the NIST OX-I samples with an assigned $\delta^{13}C$ value of –19.0‰.

SID	Cathode	Sample name	Mass (µg)	$\delta^{13}C$ ‰ VPDB	Trapping efficiency	Size (mg C)	% pMC
1	—	NIST OX-I	5941	—	—	—	—
2	18018	NIST OX-I	5731	–19.1	83.8%	0.8	104.4 ± 0.5
3	18019	NIST OX-I	5627	–19.0	80.9%	0.8	102.9 ± 0.5
4	18020	Anthracite	1258	–23.2	72.0%	0.8	0.32 ± 0.02
5	18021	Anthracite	1261	–23.1	75.1%	0.8	0.38 ± 0.02
6	18022	Anthracite	1347	–23.2	83.6%	0.8	0.20 ± 0.01
7	—	AMS BGD	3037	–16.0	—	—	—
8	—	NIST OX-I	2882	—	—	—	—
9	18024	NIST OX-I	2826	–19.1	76.1%	0.4	105.4 ± 0.5
10	18195	NIST OX-I	2803	–19.0	74.9%	0.2	105.6 ± 0.7
11	18023	Anthracite	616	–23.2	73.5%	0.4	0.38 ± 0.02
12	18196	Anthracite	603	–23.1	71.6%	0.4	0.71 ± 0.05
13	18197	Anthracite	470	–23.1	53.8%	0.2	0.77 ± 0.06
14	18025	NIST OX-I	1379	–18.9	83.4%	0.2	102.9 ± 0.5
15	18198	NIST OX-I	1693	–19.0	38.4%	0.1	102.6 ± 1.3
16	18199	NIST OX-I	1552	–19.0	64.4%	0.2	101.9 ± 0.7
17	18026	Anthracite	282	–23.0	63.5%	0.1	0.69 ± 0.05
18	18200	Anthracite	366	–23.0	63.6%	0.2	0.84 ± 0.06
19	18201	Anthracite	345	–23.1	73.2%	0.2	0.70 ± 0.05
		Anthracite	**–23.1 ± 0.08‰**		**Average of anthracite of 0.8 mg C 0.31 ± 0.01% pMC**		
		NIST OX-I	**–19.0 ± 0.08‰**				

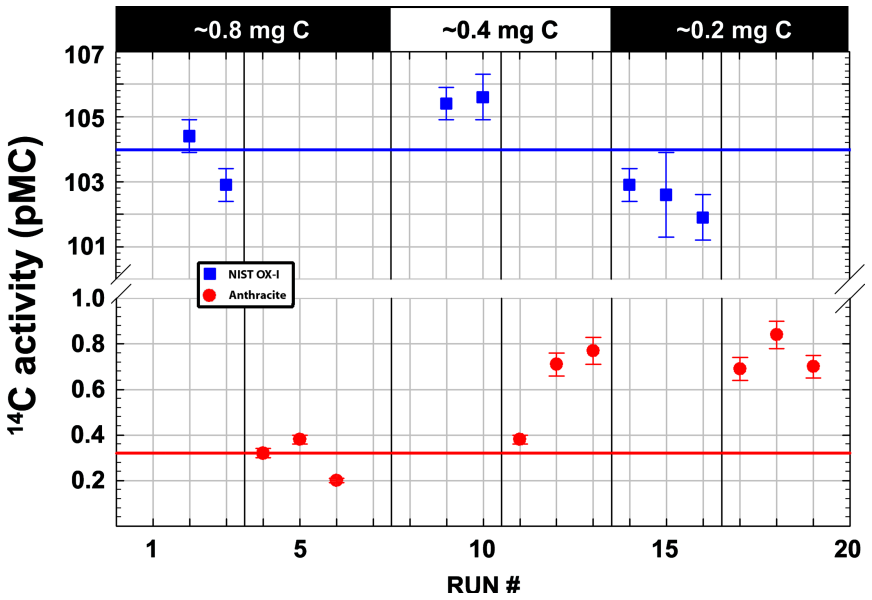

Figure 4 pMC values of alternating NIST OX-I and anthracite samples as a function of MS run number. The upper solid line represents the NIST OX-I pMC value of 103.98 and the lower solid line represents the anthracite 0.8-mg C pMC value of 0.31 ± 0.01. Note, no intersample memory effects are observed.

pump. The size dependence of the analyzed NIST OX-I samples (Figure 6) does, on the other hand, not give a simple picture. Both the NIST OX-I and anthracite samples have been measured during a period of analysis instability. The observed variability is not understood at present, but shows no systematic dependence on sample size or intersample memory effects.

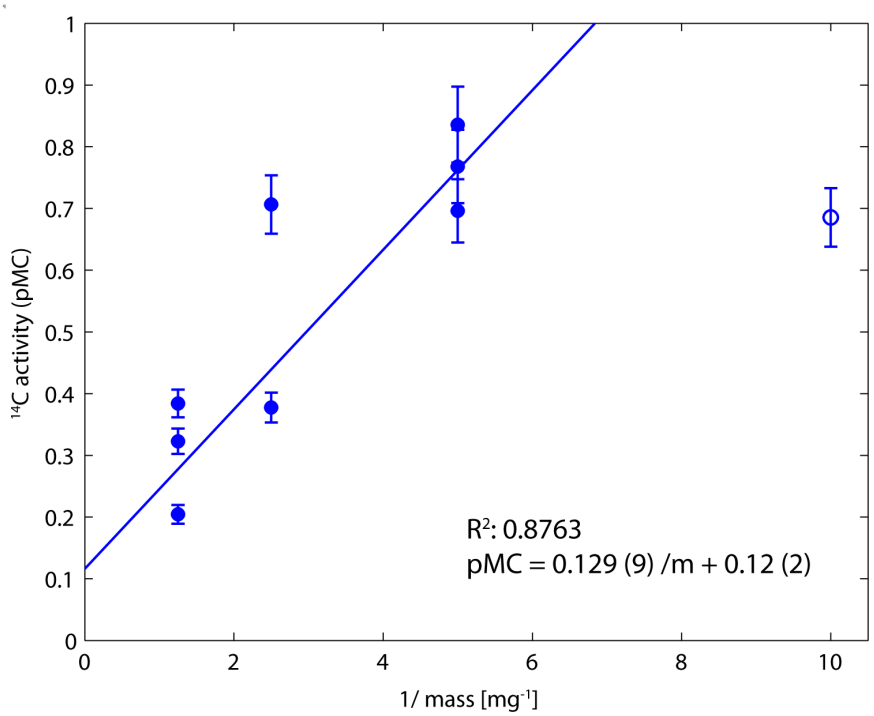

Figure 5 Size effect of analyzed anthracite samples shown as the inverse mass versus pMC values. The data are fitted to a straight line by the method of least-squares. One outlier is indicated by an open circle.

The ^{14}C background level of the anthracite is determined from the three 0.8-mg C samples to 0.31 ± 0.01 pMC, which is only slightly higher than Icelandic double spar with a pMC value of 0.20 ± 0.08 normally used for monitoring the ^{14}C background level for AMS ^{14}C analysis where the CO_2 for graphitization of the Icelandic double spar is liberated by dissolution with H_3PO_4. Bronk Ramsey and Humm (2000) reported that the tin cups used for CF-EA combustion may significantly contribute a carbon contaminant, thereby increasing the ^{14}C background level for CF-EA processed AMS samples. A test measurement of the ^{14}C content of the CF-EA tin cups was therefore carried out by processing anthracite by off-line combustion in sealed, evacuated tubes containing CuO in 3 different runs with 0, 1, and 5 tin cups added, respectively. The ^{14}C results are shown in Table 2, illustrating that the anthracite samples processed without the addition of tin cups are in excellent agreement with the 0.8-mg C CF-EA-AMS processed anthracite samples in Table 1. However, the anthracite processed with 5 tin cups added show slightly higher pMC values, indicating the CF-EA tin cups increase the pMC values by approximately 0.024 (corresponding to 0.2 µg modern carbon). Bronk Ramsey and Humm (2000) cleaned their tin cups thoroughly prior to CF-EA combustion of ^{14}C samples, a procedure which is not adopted here. However, for very small samples or very old ^{14}C samples a tin cup cleaning procedure may be successfully adopted. Aerts-Bijma et al. (2001) reported a background level of the anthracite sample of 0.24 ± 0.05 pMC, slightly lower than the anthracite value found here.

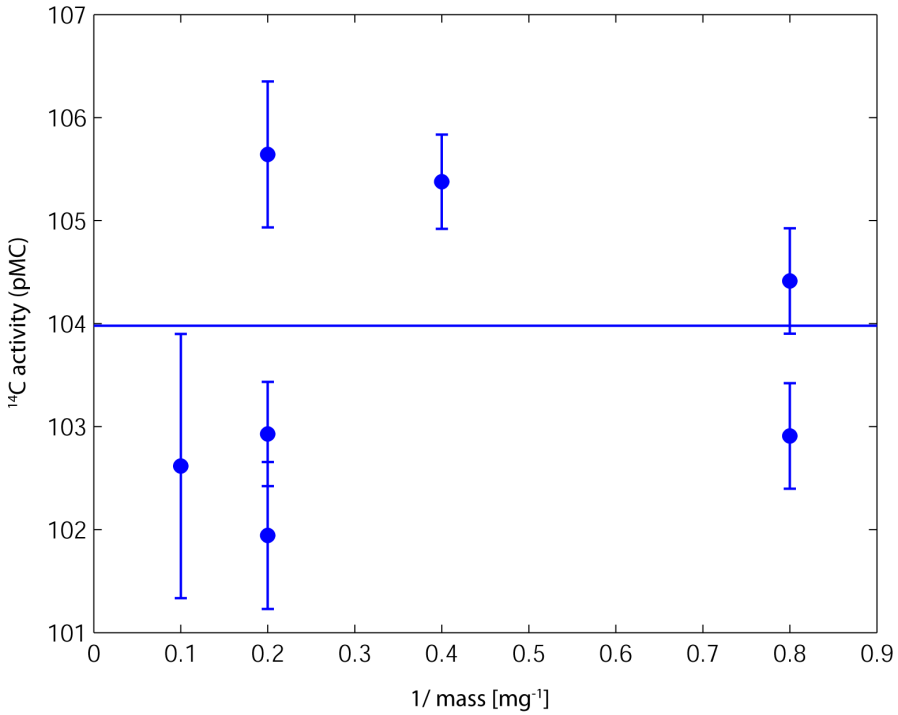

Figure 6 Size effect of analyzed NIST OX-I samples. The solid line represents the NIST OX-I pMC value of 103.98.

Table 2 Test measurement of the ^{14}C content of tin cups by using anthracite. CO_2 for graphitization is obtained by combustion in sealed, evacuated tubes containing CuO with either 0, 1, and 5 tin cups, respectively. The average pMC value of each test is shown together with χ^2 statistics, i.e. $\chi^2_{meas} \leq \chi^2$; "dev σ" denotes the deviation from the weighted mean value in terms of the standard deviation.

Anthracite			Anthracite (1× tin cup)			Anthracite (5× tin cup)		
Cathode	% pMC	dev σ	Cathode	% pMC	dev σ	Cathode	% pMC	dev σ
			17991	0.19 ± 0.02	–4.9	17992	0.35 ± 0.03	–2.7
18086	0.35 ± 0.02	2.0	18087	0.40 ± 0.02	5.5	18088	0.43 ± 0.02	–0.5
18191	0.29 ± 0.01	–1.8	18192	0.28 ± 0.01	–0.9	18193	0.47 ± 0.02	1.9
	0.32 ± 0.01	*7.2<3.8*		*0.30 ± 0.01*	*54.3<6.0*		*0.44 ± 0.01*	*11.4<6.0*

As may be observed from Table 3, the trapping efficiency is quite variable, in the range 38% to 84%. The trap efficiency was measured off-line during initial tests to ensure that the trap efficiency of the final system was high. The off-line measurements were performed manually by suspending the vial in a large dewar filled with liquid nitrogen and inserting the injection needle by hand prior to the CF-EA sample drop. The measured trap efficiency of these off-line tests was about 97% and was verified prior to the batch analysis. Consequently, the lower trap efficiencies observed during the batch analysis are ascribed to injection needle malfunction.

The problems with the injection needle will hopefully be solved in the future by adding a side hole placed just above the needle tip to prevent fragments of the septa blocking the needle. Furthermore,

Table 3 Batch run of stable isotope standards to test the accuracy and precision of the CF-EA-AMS method. The term "true" denotes the assigned value, "meas" the measured values, and "dev" the difference between the true and measured value. The accuracy is determined as the average difference between the true and measured values, and the precision is determined by as the standard deviation of the repetitive measurements of the GelA standard.

			Carbon %			δ^{13}C ‰ VPDB			Nitrogen ‰			δ^{15}N ‰ AIR		
SID	Sample name	Mass (µg)	true	meas	dev	true	meas	dev	true	meas	dev	true	meas	dev
2338	GelA	2487		41.3%	4.3%		–22.1	–0.2		16.0%	1.0%		6.0	0.4
2338	GelA	2341	45.6%	47.6%	–2.0%	–22.3	–22.2	–0.1	17.0%	18.3%	–1.4%	6.4	5.9	0.5
2338	GelA	2567		44.6%	1.0%		–22.3	0.0		17.2%	–0.2%		5.9	0.6
2345	IAEA N1	4163							21.6%	21.2%	0.4%	0.4	1.2	–0.8
3	IAEA C6	2355	44.1%	42.4%	1.7%	–10.8	–10.7	–0.1						
2341	IAEA N2	4532							20.4%	21.2%	–0.8%	20.3	20.6	–0.3
373	IAEA C7	6188		28.0%		–14.5	–14.6	0.1						
3599	IAEA N3	2478							13.9%	14.1%	–0.3%	4.7	5.0	–0.3
374	IAEA C8	5454	19.9%	21.5%	–1.6%	–18.3	–18.4	0.1						
2792	AMS BGD	2945	40.9%	42.7%	–1.8%	–16.0	–16.4	0.4	15.0%	16.0%	–1.0%	11.7	11.8	0.0
2345	IAEA N1	3731							21.6%	21.2%	0.4%	0.4	1.2	–0.8
3	IAEA C6	2732	44.1%	41.9%	2.2%	–10.8	–10.7	–0.1						
2341	IAEA N2	4039							20.4%	18.8%	1.6%	20.3	20.5	–0.2
373	IAEA C7	6001		27.4%		–14.5	–14.6	0.1						
3599	IAEA N3	3067							13.9%	12.2%	1.6%	4.7	4.7	0.0
374	IAEA C8	4943	19.9%			–18.3								
2792	AMS BGD	2749	40.9%	41.9%	–1.0%	–16.0	–16.3	0.4	15.0%	15.7%	–0.7%	11.7	11.8	–0.1
2345	IAEA N1	3693							21.6%	20.6%	1.0%	0.4	1.2	–0.8
3	IAEA C6	2537	44.1%	41.4%	2.7%	–10.8	–10.8	0.0						
2341	IAEA N2	3707							20.4%	20.7%	–0.3%	20.3	20.6	–0.3
373	IAEA C7	5932	17.5%			–14.5								
3599	IAEA N3	2499							13.9%	11.7%	2.1%	4.7	5.0	–0.3
374	IAEA C8	5529	19.9%	20.1%	–0.3%	–18.3	–18.5	0.2						
2338	GelA	2555		44.9%	0.7%	–22.3	–22.3	0.0		17.4%	–0.4%		5.8	0.6
2338	GelA	2471	45.6%	46.1%	–0.5%		–22.3	0.0	17.%	17.8%	–0.8%	6.4	5.7	0.7
2338	GelA	2248		43.3%	2.2%		–22.3	0.0		16.8%	0.2%		5.7	0.7
	Average				*0.6%*			*0.1*			*0.1%*			*0.0*
	Standard deviation				*2.0%*			*0.2*			*1.0%*			*0.5*

an improved needle holder is being produced to enable fine adjustments of the needle in the horizontal plane of the manifold bed and to ensure that the needle penetrates the exact center of both septa.

Stable Isotope Analysis

A batch of 25 stable isotope standards was analyzed to determine the precision and accuracy of the CF-EA AMS sample preparation device (see Table 3 and Figures 7, 8). The observed precision and accuracy is 0.1 ± 0.2‰ and 0.1‰, respectively, for $\delta^{13}C$ analysis and 0.0 ± 0.5‰ and 0.1‰ for $\delta^{15}N$ analysis. Hence, the elemental composition of carbon and nitrogen and the stable isotope analysis of $\delta^{13}C$ and $\delta^{15}N$ perfectly match the result expected for normal CF-EA analysis (Werner and Brand 2001). Likewise, the "AMS BGD" sample of Table 1, having a measured $\delta^{13}C$ value of –16.0‰, is in agreement with the assigned $\delta^{13}C$ value of –16.1‰ (internal $\delta^{13}C$ and ^{14}C standard). The anthracite standard has also been measured by both the normal CF-EA (–23.2 ± 0.1‰) method and by the DI method (–23.1 ± 0.2‰); hence, compared with the CF-EA-AMS analysis (Table 1), the 3 methods display excellent mutual agreement.

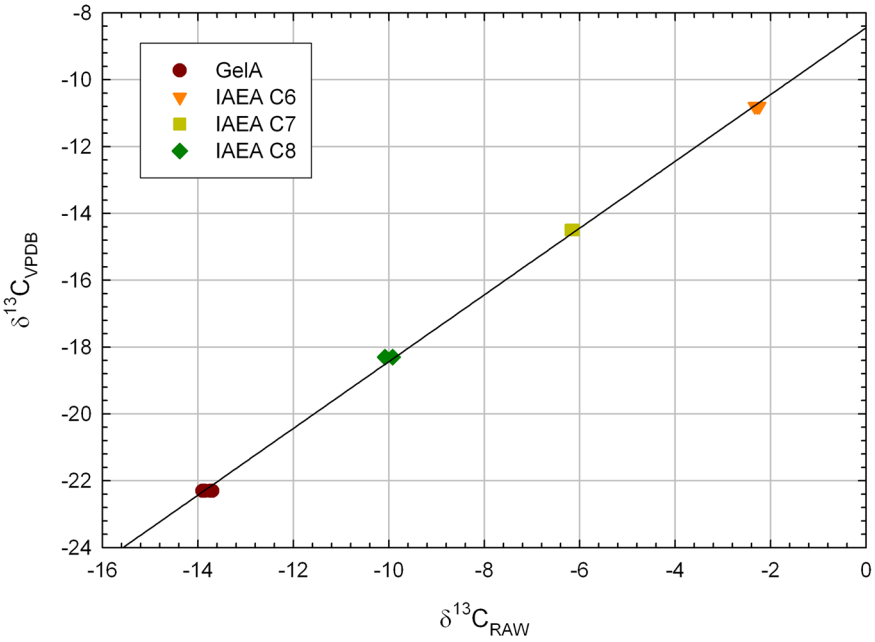

Figure 7 Raw $\delta^{13}C$ values (measured relative to machine working gas) as function of assigned (true) $\delta^{13}C$ value.

The $\delta^{13}C$ values of the three 0.8-mg C anthracite samples (Table 1; Cathode 18020, 18021 & 18022) were also determined on the cryogenically-trapped CO_2 fraction by the dual-inlet method. The $\delta^{13}C$ values obtained by the dual-inlet method all deviate less than ±0.1‰ from their respective $\delta^{13}C$ values obtained by the CF-EA-AMS method. The $\delta^{13}C$ values determined by the CF-EA-AMS and the DI method on the same CO_2 gas all mutually agree, indicating that isotopic fractionation by the splitting of the CO_2 gas is insignificant.

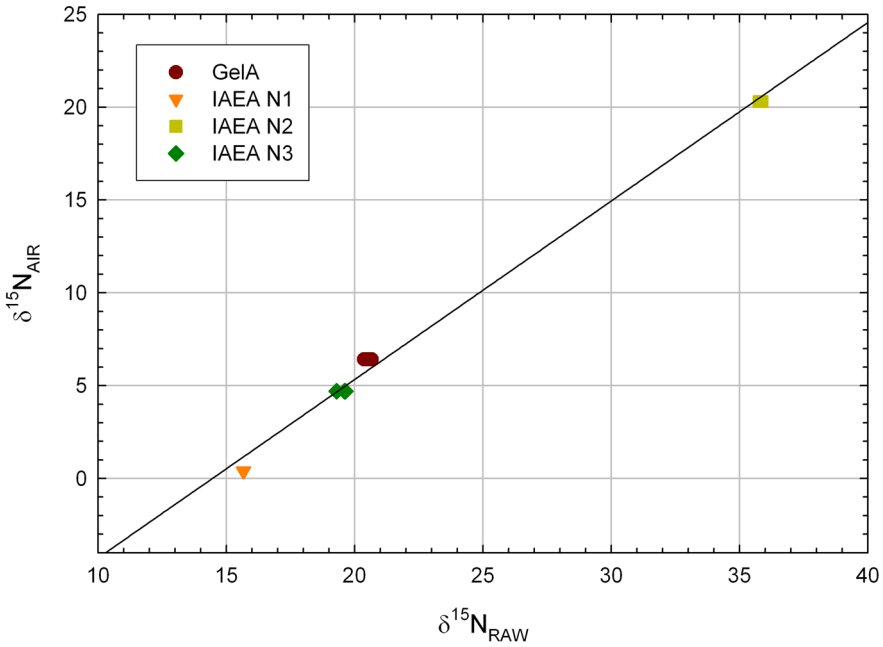

Figure 8 Raw $\delta^{15}N$ values (measured relative to machine working gas) as function of assigned (true) $\delta^{15}N$ value.

CONCLUSION

A CF-EA-AMS sample preparation system combined with stable isotope analysis of $\delta^{13}C$ and $\delta^{15}N$ has been designed and successfully tested. The system is based on a modified CF-EA and Gilson 222XL robot, enabling cryogenic trapping of CO_2. The system is under full IRMS control. A user interface is incorporated into the IRMS software, enabling easy and simple access to method parameters. Furthermore, the system is flexible, and shifting between DI applications and CF-EA-AMS applications of the Gilson robot is straightforward.

The ^{14}C background is demonstrated to be at an acceptable level, with a pMC value of 0.31 ± 0.01. Likewise, the ^{14}C measurements indicate that the contaminant carbon added during either CF-EA combustion, CO_2 trapping, and during the graphitization step are minor. The stable isotope analysis of $\delta^{13}C$ and $\delta^{15}N$ has been found to be in excellent agreement with the expected precision and accuracy of normal CF-EA isotope analysis. However, the sample analysis also revealed that the design of the needle and needle holder need to be improved before routine samples can be analyzed. Thus, more work has to be done before either small or old samples can be routinely processed with confidence.

ACKNOWLEDGMENTS

H A J Meier, H van der Plicht, A Aerts-Bijma, and the staff at the Center for Isotope Research, Groningen are thanked for fruitful discussions and for letting us have the anthracite background material. The Danish Natural Science Research Council is thanked for funding this work. C Turney and H Kjeldsen are thanked for their critical comments and suggestions to improve the manuscript.

REFERENCES

Aerts-Bijma AT, van der Plicht J, Meijer HAJ. 2001. Automatic AMS sample combustion and CO_2 collection. *Radiocarbon* 43(2A):293–8.

Allison CE, Francey RJ, Meijer HAJ. 1993. Recommendations for the reporting of stable isotope measurements of carbon and oxygen in CO_2 gas. In: Reference and intercomparison materials for stable isotopes of light elements [IAEA-TECDOC-825]. Vienna: IAEA. p 155–62.

Ambrose SH, Krigbaum J. 2003. Bone chemistry and bioarchaeology. *Journal of Anthropological Archaeology* 22(3):193–9.

Bronk Ramsey C, Humm MJ. 2000. On-line combustion of samples for AMS and ion source developments at ORAU. *Nuclear Instruments and Methods in Physics Research B* 172(1–4):242–6.

Brown TA, Southon JR. 1997. Corrections for contamination background in AMS ^{14}C measurements. *Nuclear Instruments and Methods in Physics Research B* 123(1–4):208–13.

Craig H. 1957. Isotopic standards for carbon and oxygen and correction factors for mass-spectrometric analysis of carbon dioxide. *Geochimica et Cosmochimica Acta* 12(1–2):133–49.

Filippi ML, Talbot MR. 2005. The palaeolimnology of northern Lake Malawi over the last 25 ka based upon the elemental and stable isotopic composition of sedimentary organic matter. *Quaternary Science Reviews* 24(10–11):1303–28.

Ghosh P, Brand WA. 2003. Stable isotope ratio mass spectrometry in global climate change research. *International Journal of Mass Spectrometry* 228(1):1–33.

Hatté C, Poupeau J-J, Tatman J-F, Paterne M. 2003. Development of an automated system for preparation of organic samples. *Radiocarbon* 45(3):421–30.

Hua Q, Zoppi U, Williams AA, Smith AM. 2004. Small-mass AMS radiocarbon analysis at ANTARES. *Nuclear Instruments and Methods in Physics Research B* 223–224:284–92.

Kohn MJ, Law JM. 2006. Stable isotope chemistry of fossil bone as a new paleoclimate indicator. *Geochimica et Cosmochimica Acta* 70(4):931–46.

Leach F, Quinn C, Morrison J, Lyon G. 2001. The use of multiple isotope signatures in reconstructing prehistoric human diet from archaeological bone from the Pacific and New Zealand. *New Zealand Journal of Archaeology* 23:31–98.

McNichol AP, Jull AJT, Burr GS. 2001. Converting AMS data to radiocarbon values: considerations and conventions. *Radiocarbon* 43(2A):313–20.

Morgenroth G, Kerscher H, Kretschmer W, Klein M, Reichel M, Tully T, Wrzosok I. 2000. Improved sample preparation techniques at the Erlangen AMS-facility. *Nuclear Instruments and Methods in Physics Research B* 172(1–4):416–23.

Mueller K, Muzikar P. 2002a. Correcting for contamination in AMS ^{14}C dating. *Radiocarbon* 44(2):591–5.

Mueller K, Muzikar P. 2002b. Quantitative study of contamination effects in AMS ^{14}C sample processing. *Nuclear Instruments and Methods in Physics Research B* 197(1–2):128–33.

Newsome SD, Phillips DL, Culleton BJ, Guilderson TP, Koch PL. 2004. Dietary reconstruction of an early to middle Holocene human population from the central California coast: insights from advanced stable isotope mixing models. *Journal of Archaeological Science* 31(8):1101–15.

Noe-Nygaard N, Price TD, Hede SU. 2005. Diet of aurochs and early cattle in southern Scandinavia: evidence from ^{15}N and ^{13}C stable isotopes. *Journal of Archaeological Science* 32(6):855–71.

Olsen J, Seierstad I, Vinther B, Johnsen S, Heinemeier J. 2006. Memory effect in deuterium analysis by continuous flow isotope ratio measurement. *International Journal of Mass Spectrometry* 254(1–2):44–52.

Richter J, Noe-Nygaard N. 2003. A Late Mesolithic hunting station at Agernæs, Fyn, Denmark. *Acta Archaeology* 74(1):1–64.

Stuiver M, Polach HA. 1977. Discussion: reporting of ^{14}C data. *Radiocarbon* 19(3):355–63.

Talbot MR, Jensen NB, Lærdal T, Filippi ML. 2006. Geochemical responses to a major transgression in giant African lakes. *Journal of Paleolimnology* 35(3): 467–89.

Werner RA, Brand WA. 2001. Referencing strategies and techniques in stable isotope ratio analysis. *Rapid Communications in Mass Spectrometry* 15(7):501–19.